Electrohydrodynamic direct-writing of conductor–insulator–conductor multi-layer interconnection*

Zheng Gao-Feng(郑高峰)[a], Pei Yan-Bo(裴艳博)[a)b)], Wang Xiang(王 翔)[a)], Zheng Jian-Yi(郑建毅)[a)†], and Sun Dao-Heng(孙道恒)[a)]

[a)] *Department of Mechanical and Electrical Engineering, Xiamen University, Xiamen* 361005, *China*
[b)] *School of Mechanical and Electrical Engineering, Harbin Institute of Technology, Harbin* 150001, *China*

(Received 12 September 2013; revised manuscript received 4 January 2014; published online 10 April 2014)

A multi-layer interconnection structure is a basic component of electronic devices, and printing of the multi-layer interconnection structure is the key process in printed electronics. In this work, electrohydrodynamic direct-writing (EDW) is utilized to print the conductor–insulator–conductor multi-layer interconnection structure. Silver ink is chosen to print the conductor pattern, and a polyvinylpyrrolidone (PVP) solution is utilized to fabricate the insulator layer between the bottom and top conductor patterns. The influences of EDW process parameters on the line width of the printed conductor and insulator patterns are studied systematically. The obtained results show that the line width of the printed structure increases with the increase of the flow rate, but decreases with the increase of applied voltage and PVP content in the solution. The average resistivity values of the bottom and top silver conductor tracks are determined to be 1.34×10^{-7} Ω·m and 1.39×10^{-7} Ω·m, respectively. The printed PVP layer between the two conductor tracks is well insulated, which can meet the insulation requirement of the electronic devices. This study offers an alternative, fast, and cost-effective method of fabricating conductor–insulator–conductor multi-layer interconnections in the electronic industry.

Keywords: electrohydrodynamic direct-writing, multi-layer interconnection, all inkjet printing, jet printing

PACS: 61.30.Pq, 81.16.–c, 85.40.–e, 94.20.Ss **DOI:** 10.1088/1674-1056/23/6/066102

1. Introduction

The fast and low-cost direct printing of a microstructure is one of the key research areas in the all-printed electronic industry, which has attracted considerable attention.[1,2] The inkjet printing technology has demonstrated a great potential of application in the all-printed electronic industry due to its features of high efficiency, low-cost, low waste, and non-contact process.[3,4] Compared with the traditional thin layer deposition techniques, such as photolithography,[5,6] electrochemical deposition,[7,8] and thermal evaporation,[9,10] inkjet printing has better compatibility with various materials.[11,12] Polymer, metal, semiconductor, and ceramics solutions can be printed on the solid or flexible substrate by inkjet printing, which provides to be a decent way to fabricate all-printed electronic devices.[13] With the help of a motion platform, complex functional patterns can be inkjet-printed without a stencil plate. Furthermore, the inkjet head has no contact with the substrate and will not damage the pre-fabricated structure during the printing process,[14,15] so that this technique can be applied to the printing of complex three-dimensional (3D) devices with multiple functional layers.

Electrohydrodynamic direct-writing (EDW) is a novel inkjet printing technology stemming from EHD printing which utilizes an external electric field to elongate the solution into a Taylor cone and generate a charged jet from the tip of the Taylor cone.[16,17] In the EDW process, the stable straight jet is utilized to directly write micro/nano structures precisely. By shortening the distance from the spinneret to the collector,[18–20] the instability and whipping of the charged jet in EHD printing is overcome. The charged jet is ejected from the tip of the Taylor cone, so the diameter of the jet is not limited by the inner diameter of the spinneret. Compared with traditional inkjet printing technology using internal pressure, such as the thermal inkjet and piezoelectric inkjet, EDW is more capable of directly printing micro/nano structures with a smaller line width. The minimal line width of micro/nano structures directly written by EDW is 50 nm. EDW is a direct and efficient technology to print micro/nano structures with high resolution patterns, which meets the demand in the development of all-printed electronics.

The interconnection is a basic component of the integrated circuit. It plays an important role in increasing the integration density and reducing the size of electronic systems.[21,22] At present, the post-removing process is the main process used to fabricate printed circuit board. Multi-layer boards and thru-hole interconnections are the most common methods to increase the circuit integration density.[23,24] However, these methods come with an increased process complexity and a higher cost. As an alternative, multi-layer over-

*Project supported by the Key Program of the National Natural Science Foundation of China (Grant No. 51035002), the National Natural Science Foundation of China (Grant No. 51305373), and the Specialized Research Fund for the Doctoral Program of Higher Education of China (Grant No. 20120121120035).

†Corresponding author. E-mail: zjy@xmu.edu.cn

© 2014 Chinese Physical Society and IOP Publishing Ltd

lapped printing of different functional materials has demonstrated significant advantages,[25,26] by which 3D multi-layer devices as well as flat interconnections can be fabricated on the substrate quickly without introducing an etching process. Conductor, insulator, and semiconductor materials[27–30] can be printed layer by layer to construct a multi-layer interconnection directly.

In this paper, EDW is used to inkjet-print a conductor–insulator–conductor multi-layer interconnection, which consists of a bottom conductor track, an insulator layer, and a top conductor track. The conductor layer is printed with silver ink, and the insulator layer with a polyvinylpyrrolidone (PVP) solution. The influences of the process parameters on the line width and uniformity of the printed micro-pattern are discussed. Furthermore, the resistivity values of the conductor layer and the insulator layer are studied.

2. Experimental details

2.1. Materials

A commercial silver ink (TEC-IJ-040, InkTec), with a viscosity of 9 cPs∼15 cPs, a surface tension of 30 dynes/cm∼32 dynes/cm, a density of 1.07 g/cm^3 at 25 °C and containing 20-wt% silver, was used to print the conductor layer. Polyvinylpyrrolidone (PVP, $M_W = 1.3 \times 10^6$ g/mol, Acros Organics) was selected to print the insulator layer. The PVP was dissolved in a mixed solution of deionized water and ethanol ($v : v = 3 : 2$), and the PVP solution content value ranged from 6 wt% to 14 wt%.

Glass slides with a thickness of 130 μm (18 mm × 18 mm; Sail Brand, China) were used as the collector. Before the printing experiment, the collector was ultrasonically cleaned in acetone for 20 min, and then in the deionized water for 10 min. After being cleaned, the glass slides were dried in the hot air blower for 10 min.

2.2. EDW experiment process

In this work, the experimental setup consisted of a spinneret, a power supply, a syringe pump, a collector, an X–Y motion platform and a high-speed camera, as illustrated in Fig. 1. A stainless steel capillary spinneret (i.d. = 60 μm, o.d. = 190 μm) was connected to the anode of the high-voltage DC power supply (Dongwen DW-P403, China). The silver link and polymer solution were supplied by the syringe pump (Havard 11 Pico Plus, USA) to the spinneret. The glass slide was located on the grounded X–Y motion platform (Googol GXY1515GT4, China) vertically below the spinneret as a collector. The motion track of the platform was controlled by a host computer.

In the EDW process, droplets at the outlet of the spinneret were elongated by the electric field force generated by the applied voltage. When the electric field force overcomes the surface tension, a fine jet is created. The jet was accelerated by the electrical field force and then deposited on the collector to form micro/nano structures. The process of cone jet ejection was observed and recorded by a high-speed camera (GX-1.NAC, Japan). An optical microscope (Mitutoyo) was employed to observe the deposited patterns. The resistance of the printed EDW pattern was measured by a digital multimeter (PXI-4072, NI).

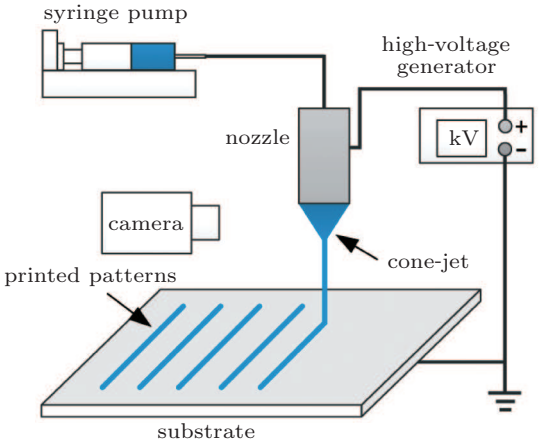


Fig. 1. (color online) Schematic diagram of EDW apparatus.

3. Results and discussion

3.1. Printing of the conductor pattern

3.1.1. Applied voltage

The silver ink is utilized to print conductor tracks, and the printed conductor tracks under different applied voltages are shown in Fig. 2(a). The stand-off height between the spinneret and the collector is 250 μm. The flow rate is 20 μL/h, and the collector velocity is 10 mm/s. The obtained results demonstrate that the line width of the printed conductor track increases from 158 μm to 340 μm as the applied voltage increases from 1.0 kV to 1.5 kV as shown in Fig. 2(b).

Youn *et al.*[16] reported that higher applied voltages lead to higher axial and radical electric fields, which weaken the stability and increase the diameter of the silver ink jet. Both the electric field intensity and the electric field force increase with the increase of applied voltage, therefore more ink is ejected from the spinneret. On the other hand, higher applied voltages and higher electric field intensity induce more charges to accumulate on the Taylor cone surface. When the EHD jet is ejected from the tip of the Taylor cone, it also carries away the accumulated charges. The charge density of the jet is the key factor that dominates the motion and rheological

behaviors.[31] Li *et al.*[32] reported that the Coulomb repulsion played the main role in the morphology of EHD printed micro/nano structures. The silver ink tended to form micro/nano droplets under high voltage electrical fields due to its low viscosity and surface tension. Micro/nano droplets that stem from the charged jet will be scattered by the Coulomb repulsion force and deposited as satellite dots around the printed pattern, so the higher the applied voltage, the more satellite dots and the larger distribution zone it brings about. Wang *et al.*[19] reported that the satellite dots scattering area around the printed pattern, as well as the line width, increased with the increase of the applied voltage. The line width error distribution range increases along with the applied voltage, due to the larger scattering area of satellite dots as shown in Fig. 2(b). The scattering deposition of satellite dots is an uncertain factor that influences the line width, uniformity, density, and conductivity of the printed conductor pattern.

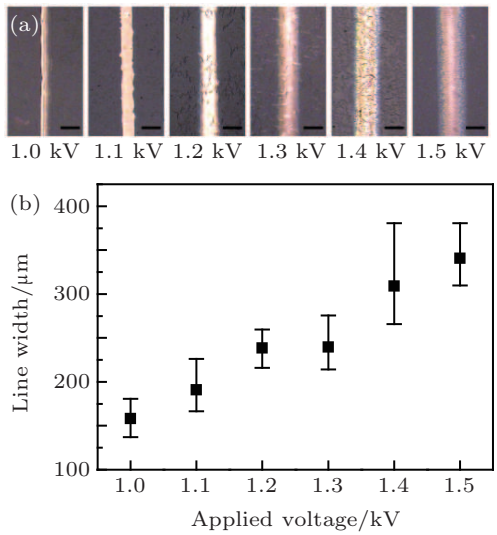


Fig. 2. (color online) Influences of applied voltages on the inkjet printed tracks. (a) Inkjet printed conductor tracks under different applied voltages (scale bar represents 250 μm); (b) relationship between the line width of the conductor structure and the applied voltage. The stand-off height, flow rate, and collector velocity are 250 μm, 20 μL/h, and 10 mm/s, respectively. The silver ink contains 20-wt% silver.

3.1.2. Flow rate

The inkjet printed conductor tracks under different flow rates are shown in Fig. 3(a). The voltage applied to the spinneret is 1.1 kV, and the flow rate varies from 10 μL/h to 40 μL/h. The increased flow rate leads to a smaller Taylor cone angle and a larger jet diameter, and then micro/nano tracks with a wider line width can be printed. The curve depicted in Fig. 3(b) demonstrates that the line width increases from 182 μm to 293 μm with the increase of flow rate from 10 μL/h to 40 μL/h. The experimental results show that smaller applied voltages and lower flow rates are helpful to fabricate uniform conductor tracks with smaller values of line width, less satellite dots, and better compactness.

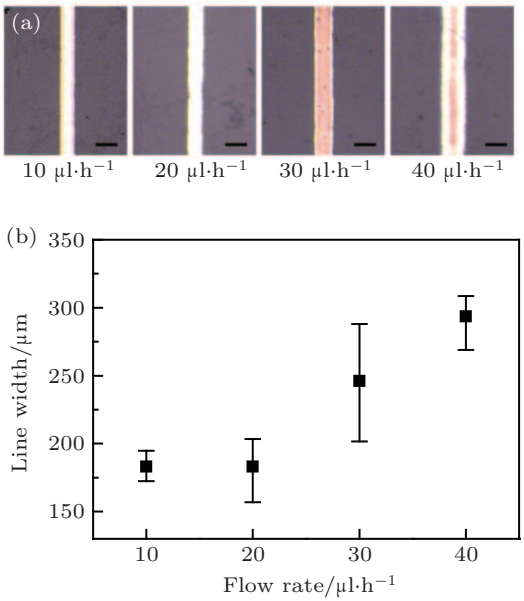


Fig. 3. (color online) Influences of flow rate on the inkjet printed tracks. (a) Printed conductor tracks under different flow rates (scale bar represents 250 μm); (b) relationship between the line width of the conductor structure and the flow rate. The stand-off height, applied voltage, and collector velocity are 250 μm, 1.1 kV, and 10 mm/s, respectively. The silver ink contains 20-wt% silver.

3.2. Printing of the insulator pattern

3.2.1. Applied voltage

When the applied voltage ranges from 1.8 kV to 2.3 kV, a stable single jet is ejected from the spinneret, as shown in Fig. 4(a). The stand-off height is 1.5 mm, the PVP content value in the solution is 12 wt%, the solution is pumped at a constant flow rate of 30 μL/h and the collector velocity is 20 mm/s. The minimal applied voltage for generating a stable jet ejection of the polymer solution is 1.8 kV. Under the lower applied voltage, surface tension plays a dominant role in the rheological behaviors of the EHD jet. Therefore, the EHD jet tends to shrink and deposit in a bead-on-string pattern on the collector, as shown in Fig. 4(a). The charged jet is stretched thinner by a higher electrical field force as the applied voltage increases. With the elongation of the EHD jet, the distance between two contiguous beads on the bead-on-string pattern decreases.

A higher applied voltage leads to a higher surface charge density on the Taylor cone and a larger jet diameter, and the higher charge repulsive force will introduce more uncertainties to disturb the positioning precision of the printed pattern. When the applied voltage is higher than 2.3 kV, the EHD charged jet is furcated into multi-jets due to the higher charge density and charge repulsive force. When the applied voltage is between 2.4 kV and 2.6 kV, the bead-on-string pattern becomes a continuous line pattern, but there are more tiny disorderly distributed satellite dots deposited around the printed line, as shown in Fig. 4(a). The curve of the line width versus the applied voltage is shown in Fig. 4(b). Before the furcation,

the axial electric force plays a major role in forming the jet and in reducing the jet diameter. A higher applied voltage leads to a larger electrical field force, which stretches the polymer solution into a finer jet. When the applied voltage rises from 1.8 kV to 2.3 kV, the line width of the printed pattern decreases from 91.43 μm to 69.18 μm accordingly.

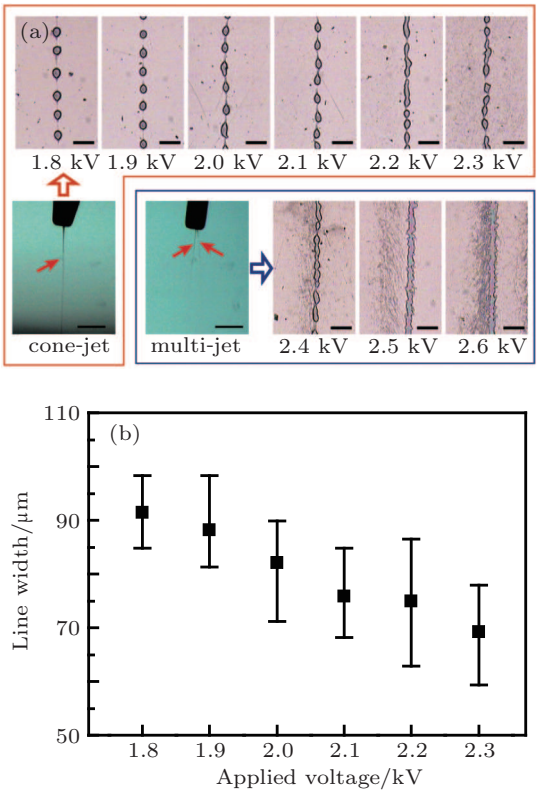


Fig. 4. (color online) Influences of the applied voltage on the inkjet insulator structure. (a) Inkjet printed insulator structures under different applied voltages (scale bar represents 250 μm); (b) relationship between the line width of the insulator structure and the applied voltage. The stand-off height, PVP content, flow rate, and collector velocity are 1.5 mm, 12 wt%, 30 μL/h, and 20 mm/s, respectively.

3.2.2. Flow rate

When the flow rate is increases from 10 μL/h to 50 μL/h, the ejection mode changes from drips to a jet, and the printed pattern also changes from the bead-on-string pattern into a continuous line, as shown in Fig. 5(a). In the experiment, the stand-off height, PVP content, applied voltage, and collector velocity are set to be 1.5 mm, 12 wt%, 1.9 kV, and 20 mm/s, respectively. The line width of the printed PVP micro-structure decreases from 120 μm to 60 μm as the flow rate increases from 10 μL/h to 50 μL/h. When the flow rate reaches 50 μL/h, a stable Taylor cone and the cone jet mode are formed, under which micro-structures can be printed smoothly. The diameter of the EHD jet increases along with the flow rate, so does the line width of the printed structure. The line width of the printed PVP micro-structure increases from 60 μm to 90 μm, as the flow rate increases from 50 μL/h to 90 μL/h.

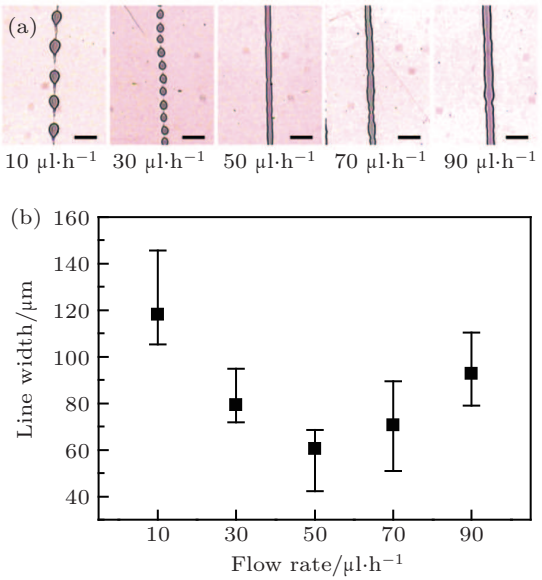


Fig. 5. (color online) Influences of the flow rate on the inkjet insulator structure. (a) Printed insulator structures under different flow rates (scale bar represents 250 μm); (b) relationship between the line width of the insulator structure and the flow rate. The stand-off height, PVP content, applied voltage, and collector velocity are 1.5 mm, 12 wt%, 1.9 kV, and 20 mm/s, respectively.

3.2.3. PVP content in solution

The insulator patterns printed with different PVP content values in solutions are shown in Fig. 6(a). As the PVP content value in the solution increases from 6 wt% to 14 wt%, the printed pattern turns into beads due to the higher solution viscosity. A PVP solution with a lower polymer content has a higher fluidity and a lower viscosity, which is difficult to stretch into a Taylor cone and a fine jet.[33] The liquid jet spreads into a pattern with a wider line width when it is deposited on the substrate. A PVP solution with a higher polymer content value is stretched into an apparent Taylor cone and further into a fine jet. Thus, when the PVP content value increases from 6 wt% to 10 wt%, the line width drops off dramatically from 156 μm to 70 μm as shown in Fig. 6(b). When the PVP content value in the solution is higher than 10 wt%, the surface tension acts as a key factor to determine the rheological behavior of the EHD jet. A higher viscosity hinders the rheology and elongation of the charged jet, so a higher solution viscosity leads to a larger jet diameter. The line width of the printed PVP pattern increases from 70 μm to 80 μm, when the PVP content value in the solution increases from 10 wt% to 14 wt%, as demonstrated in Fig. 6(b). The liquid jet tends to shrink into droplets under the solution surface tension, therefore the continuous line pattern is converted into a droplet pattern when the PVP content value in the solution is higher than 12 wt%, which is shown in Fig. 6(a).

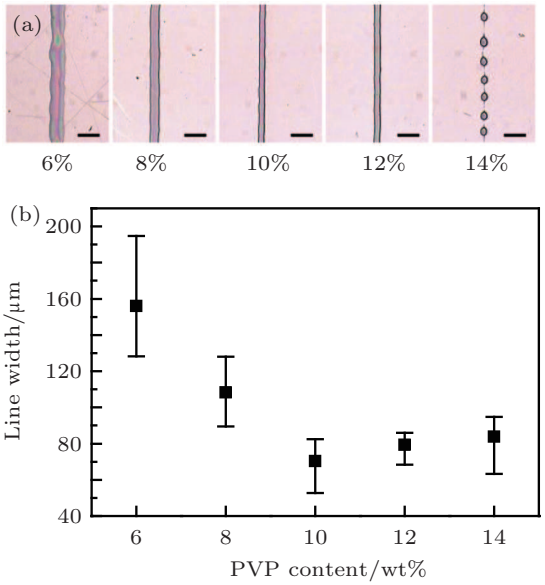


Fig. 6. (color online) Influences of PVP content on inkjet insulator structures. (a) Printed insulator structures from different PVP contents in the solution (scale bar represents 250 μm); (b) relationship between the line width of the conductor structure and the PVP content. The stand-off height, applied voltage, flow rate, and collector velocity are 1.5 mm, 1.9 kV, 30 μL/h, and 20 mm/s, respectively.

3.3. Printing of the multi-layer interconnection structure

The schematic diagram of the multi-layer interconnection structure is shown in Fig. 7(a), which comprises a bottom silver track, an insulator layer, and a top silver track. The method of fabricating multi-layer interconnection is described as follows.

(i) Silver ink EHD printing for the bottom conductor track: the stand-off height, applied voltage, and flow rate are 250 μm, 1.2 kV, and 20 μL/h, respectively.

(ii) The bottom silver track is sintered at 150 °C for 10 min to increase the conductivity.

(iii) PVP solution EHD printing for the insulator layer: the PVP content value in the solution, stand-off height, applied voltage, and flow rate are 6 wt%, 1.5 mm, 2.5 kV, and 30 μL/h, respectively.

(iv) The insulator layer is dried in air for 3 hr to ensure the full removal of the solvent.

(v) Silver ink EHD printing for the top conductor track.

(vi) The multi-layer interconnection is sintered (at 150 °C for 10 min) to increase the conductivity of the top silver track.

The complete printed structure of multi-layer interconnection is illustrated in Fig. 7(b). There are two electrodes located at the end of the bottom silver track and the top silver track, respectively. A voltage (0 V ∼ 20 V) is applied to the electrodes to measure the electrical characteristics of the printed pattern. The relationship between current through the printed pattern and the applied voltage is shown in Fig. 7(c). With the voltage increasing from 0 V to 20 V, the current on the bottom silver track rises from 0 A to 2.42 A, and that of the top silver track increases from 0 A to 2.28 A. Thus, the bottom silver track and the top silver track have average resistance values of 8.357 Ω and 8.827 Ω, respectively. When the voltage is applied between the bottom silver track and the top silver track, the current from one conductor track through the insulator layer to the other (called CIC) is also shown in Fig. 7(c). Experimental results show that the insulator layer has a high enough resistance to insulate the bottom silver track from that on the top.

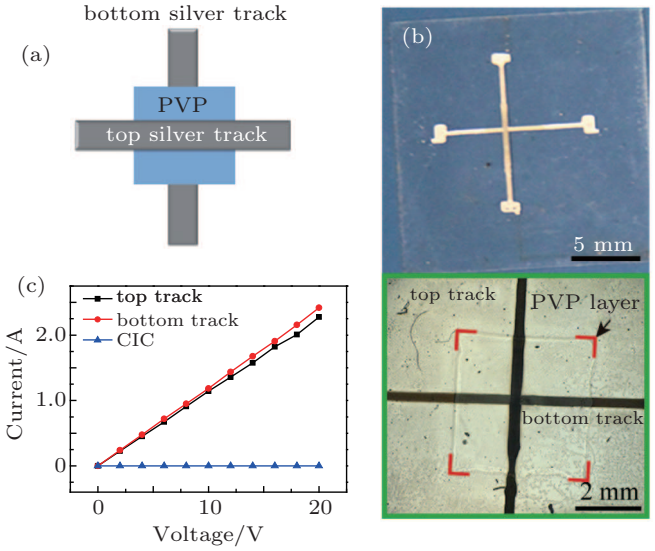


Fig. 7. (color online) Inkjet printed multi-layer interconnection and test results of electrical characteristics. (a) Schematic diagram of a multi-layer interconnection; (b) the printed multi-layer interconnection; (c) electrical characteristics of the multi-layer interconnection.

The length, average thickness, and line width of the printed bottom silver track are measured to be 10 mm, 558 nm, and 288 μm, respectively. In addition, the maximum line width of the printed bottom silver track is 321 μm and the minimum line width is 253 μm. The printed insulator layer has an average thickness value of 1.12 μm. The top silver track is printed over the insulator layer, of which the average thickness value, line width, and length are 545 nm, 287 μm, and 10 mm, respectively. Owing to the influences of the surface roughness on the pre-deposited bottom silver track and the insulator layer, the stand-off height fluctuates in the printing process, and the printed top silver track has a lower uniformity than the bottom one. On the other hand, the insulator layer also changes the electric field above the collector, which is a key factor to determine the line width. The maximum line width of the top silver track increases to 350 μm, while the minimum line width decreases to 235 μm under the same parameters.

The calculated resistivity of the bottom silver track is 1.33×10^{-8} Ω·m, which is approximately 8.4 times that of the theoretical resistivity of bulk silver, and that of the top silver track is 1.39×10^{-7} Ω·m, 8.7 times that of the theoretical resistivity of bulk silver.

4. Conclusions

In this paper, EHD printing is utilized to fabricate the conductor–insulator–conductor multi-layer interconnection. A commercial silver ink is used to print the conductor track, and a PVP solution is used to print the insulator layer. The effects of printing process parameters on printing performances of silver ink and the PVP solution are investigated, respectively. The line width of the printed silver track increases with the increase of the applied voltage and flow rate, while that of the printed PVP pattern decreases with the increase of the applied voltage and PVP content in the solution. Lower flow rate leads to the drip ejection mode while a higher flow rate is beneficial to the formation of a Taylor cone. The jet diameter and the line width of the printed track increase with the increase of the flow rate. A conductor–insulator–conductor multi-layer interconnection structure is fabricated successfully through EHD printing. The resistivity values of the bottom and top printed silver tracks are 1.34×10^{-7} Ω·m and 1.39×10^{-7} Ω·m, respectively. The average thickness of the PVP insulation layer is 1.12 μm, which demonstrates excellent insulation characteristics between the bottom and top silver tracks.

This study may improve the process controllability of insulating and conductive material printing, and offer an alternative way to fabricate multi-layer interconnections for all-printed electronic devices of the next generation.

References

[1] Lee S, Kim J, Choi J, Park H, Ha J, Kim Y, Rogers J A and Paik U 2012 *Appl. Phys. Lett.* **100** 102108

[2] Khan S, Doh Y H, Khan A, Rahman A, Choi K H and Kim D S 2011 *Curr. Appl. Phys.* **11** S271

[3] Alexander Lange, Andreas Hollaender and Michael Wegener 2013 *Mater. Sci. Eng. B: Adv.* **178** 299

[4] Hwang M S, Jeong B Y, Moon J, Chun S K and Kim J 2011 *Mater. Sci. Eng. B: Adv.* **176** 1128

[5] Kim W J, Kim S J, Cartwright A N and Prasad P N 2013 *Nanotechnology* **24** 065302

[6] Ye J S, Wang J Z, Huang Q L, Dong B Z, Zhang Y and Yang G Z 2013 *Chin. Phys. B* **22** 034201

[7] Alikhanzadeh-Arani S, Almasi-Kashi M and Ramazani A 2013 *Curr. Appl. Phys.* **13** 664

[8] Zhang P Z, Li R S, Pan X J and Xie E Q 2013 *Chin. Phys. B* **22** 058106

[9] Lee H, Park S, Lee J, Lee Y, Shin D, Jeong K and Yi Y 2013 *Appl. Phys. Lett.* **102** 033302

[10] Song D M, Tang Z X, Zhao L, Sui Z, Wen S C and Fan D Y 2013 *Chin. Phys. Lett.* **30** 044206

[11] Singh M, Haverinen H M, Dhagat P and Jabbour G E 2010 *Adv. Mater.* **22** 673

[12] Lee J, Chung S, Song H, Kim S and Hong Y 2013 *J. Phys. D: Appl. Phys.* **46** 105305

[13] Lau P H, Takei K, Wang C, Ju Y, Kim J, Yu Z, Takahashi T, Cho G and Javey A 2013 *Nano. Lett.* **13** 3864

[14] Chung S, Kim S O, Kwon S K, Lee C and Hong Y 2011 *IEEE Electron. Dev. Lett.* **32** 1134.

[15] Ding Y, Huang E, Lam K S and Pan T 2013 *Lab. Chip.* **13** 1902

[16] Youn D H, Kim S H, Yang Y S, Lim S C, Kim S J, Ahn S H, Sim H S, Ryu S M, Shin D W and Yoo J B 2009 *Appl. Phys. A: Mater.* **96** 933

[17] Mishra S, Barton K L, Alleyne A G, Ferreira P M and Rogers J A 2010 *J. Micromech. Microeng.* **20** 095026

[18] Xu L and Sun D 2013 *Appl. Phys. Lett.* **102** 024101

[19] Wang X, Xu L, Zheng G, Cheng W and Sun D 2012 *Sci. China: Technol. Sci.* **55** 1603

[20] Zheng J, Long Y Z, Sun B, Zhang Z H, Shao F, Zhang H D, Zhang Z M and Huang J Y 2012 *Chin. Phys. B* **21** 048102

[21] Xu S, Zhang Y, Cho J, Lee J, Huang X, Jia L, Fan J A, Su Y, Su J, Zhang H, Cheng H, Lu B, Yu C, Chuang C, Kim T, Song T, Shigeta K, Kang S, Dagdeviren C, Petrov I, Braun P V, Huang Y, Paik U and Rogers J 2013 *Nat. Commun.* **4** 1543

[22] Jain N, Durcan C A, Jacobs-Gedrim R, Xu Y and Yu B 2013 *Nanotechnology* **24** 355202

[23] Ghassemi N and Wu K 2012 *IEEE T. Anten. Propag.* **60** 4432

[24] Nam S, Jiang X, Xiong Q, Ham D and Lieber C M 2009 *Proc. Natl. Acad. Sci.* **106** 21035

[25] Janeczek K, Kozioł G, Jakubowska M, Araźna A, Młożniak A and Futera K 2013 *Mater. Sci. Eng. B: Adv.* **178** 511

[26] Xu Z and Lu J Q 2013 *IEEE T. Semiconduct. M.* **26** 23

[27] Tseng H Y and Subramanian V 2011 *Org. Electron.* **12** 249

[28] Rahman K, Mustafa M, Muhammad N and Choi K 2012 *Electron. Lett.* **48** 1261

[29] Kim S H, Hong K, Xie W, Lee K H, Zhang S, Lodge T P and Frisbie C D 2012 *Adv. Mater.* **25** 1822

[30] Kim S, Won S, Sim G D, Park I and Lee S B 2013 *Nanotechnology* **24** 085701

[31] Kim B, Nam H, Kim S J, Sung J, Joo S W and Lim G 2011 *J. Micromech. Microeng.* **21** 075020

[32] Li M M, Long Y Z, Yin H X and Zhang Z M 2011 *Chin. Phys. B* **20** 048101

[33] Huang Y F, Xu L, Zheng G F, Liu Z P and Sun D H 2010 *Chinese Journal of Sensors and Actuators* **23** 918